

# Reducing Operational Hurricane Intensity Forecast Errors during Eyewall Replacement Cycles

JAMES P. KOSSIN

*NOAA/National Centers for Environmental Information/Center for Weather and Climate, Asheville, North Carolina*

MARK DEMARIA

*NOAA/National Hurricane Center, Miami, Florida*

(Manuscript received 23 September 2015, in final form 28 January 2016)

## ABSTRACT

Eyewall replacement cycles (ERCs) are fairly common events in tropical cyclones (TCs) of hurricane intensity or greater and typically cause large and sometimes rapid changes in the intensity evolution of the TC. Although the details of the intensity evolution associated with ERCs appear to have some dependence on the ambient environmental conditions that the TCs move through, these dependencies can also be quite different than those of TCs that are not undergoing an ERC. For example, the Statistical Hurricane Prediction Scheme (SHIPS), which is used in National Hurricane Center operations and provides intensity forecast skill that is, on average, equal to or greater than deterministic numerical model skill, typically identifies an environment that is not indicative of weakening during the onset and subsequent evolution of an ERC. Contrarily, a period of substantial weakening does typically begin near the onset of an ERC, and this disparity can cause large SHIPS intensity forecast errors. Here, a simple model based on a climatology of ERC intensity change is introduced and tested against SHIPS. It is found that the application of the model can reduce intensity forecast error substantially when applied at, or shortly after, the onset of ERC weakening.

## 1. Introduction

Sitkowski et al. (2011) created a database of eyewall replacement cycle (ERC) events using satellite microwave imagery, radar imagery, and flight-level aircraft reconnaissance data to identify the onset of an ERC. They then used radial profiles of aircraft flight-level tangential wind to capture the evolution of the inner and outer wind maxima and their radii during the ERC. The use of the aircraft data was motivated mainly by a desire to 1) capture intensity changes on shorter time scales than the 6-hourly best-track<sup>1</sup>

resolution and 2) quantitatively capture not just the evolution of the absolute maximum wind (as recorded in the best-track dataset), but also the evolution of the primary and secondary wind maxima separately. Additionally, this allowed them to capture the radial contraction/expansion of the two wind maxima. Kossin and Sitkowski (2012) then used this information to create simple statistical models that could estimate the evolution of the wind maxima and their radii based on environmental and satellite data.

The flight-level data and the models of Kossin and Sitkowski (2012) are well suited to capturing and predicting details of wind structure evolution associated with ERCs, but they are not optimal for addressing operational requirements, which focus mostly on forecasting the maximum wind regardless of its position relative to the storm center and not the broader details of the wind structure and interplay between the inner and outer wind maxima. Also, it is the best-track data, which primarily provide intensity and storm center position estimates, that are used to ultimately measure forecast error and skill. Here, we will direct our focus more specifically toward operational intensity forecasting needs.

---

<sup>1</sup>The best-track record, known as the HURDAT record in the North Atlantic (Landsea and Franklin 2013), comprises 6-hourly best estimates of tropical cyclone location and intensity (measured as the maximum sustained surface wind). The HURDAT data are also part of the International Best Track Archive for Climate Stewardship (IBTrACS; Knapp et al. 2010).

---

*Corresponding author address:* James Kossin, NOAA/Cooperative Institute for Meteorological Satellite Studies, 1225 W. Dayton St., Madison, WI 53706.  
E-mail: james.kossin@noaa.gov

The three phases of an ERC, as defined by Sitkowski et al. (2011), include an initial phase where intensification is continuing but the rate is slowing, a weakening phase, and a reintensification phase. These phases were based entirely on the coevolution of the inner and outer wind maxima. The weakening phase is arguably the most important from a forecasting point of view because the intensification rate typically changes dramatically at its onset, from positive to negative, and weakening can persist for 12 h or longer (Willoughby et al. 1982; Sitkowski et al. 2011). Furthermore, the weakening phase is unique in that it is apparently driven mostly by processes internal to the tropical cyclone and not dominated by environmental factors, as will be discussed below. Comparatively, the intensification leading up to the onset of an ERC, and the intensity evolution after the completion of an ERC, are apparently controlled largely by the environment. In this respect, the weakening phase of an ERC describes a brief and idiosyncratic period in which the usual environmental controls of intensity are substantially countermanded. This motivates an alternative model that can be applied as needed to complement the existing models. Here, a model is constructed that uses a climatology of intensity evolution during and after the onset of the weakening phase of an ERC to form a simple predictive model.

## 2. Model construction and testing

We use North Atlantic best-track data (HURDAT) collected in 13 storms that underwent an ERC, or multiple ERCs, while being actively sampled by aircraft reconnaissance. Best-track intensity estimates that utilize aircraft data (referred to here as recon-anchored best track) provide a reasonable proxy for ground truth (e.g., Knaff et al. 2010), albeit with the inherent temporal smoothing applied to the 6-hourly best-track data. Because the weakening phase of an ERC can have a relatively long duration, there is an expectation that the weakening will manifest itself in some way in the best track; however, in the absence of in situ measurements, there is uncertainty in how well the best track can capture the transient weakening period. For example, it is not clear how intensity estimates based on remote sensing methods such as the Dvorak technique (Velden et al. 2006) are affected by ERCs. Our choice to restrict our analysis to ERC events that occurred during active aircraft reconnaissance places significant limitations on our available sample size, but greatly reduces the uncertainty in how well the best track is capturing transient intensity fluctuations during an ERC.

Table 1 lists the storms and the dates and times of onset of the weakening phase of 19 ERC events, as manifested in the recon-anchored best-track data. The

TABLE 1. ERC events during active aircraft reconnaissance and the time and date of the onset of the ERC weakening phase, as captured by the best-track dataset (HURDAT).

Storm	Time and date
Luis	0000 UTC 5 Sep 1995
Erika	1800 UTC 9 Sep 1997
Georges	0600 UTC 20 Sep 1998
Floyd	1200 UTC 13 Sep 1999
Fabian	1800 UTC 2 Sep 2003
Isabel	1800 UTC 14 Sep 2003
Frances	1200 UTC 29 Aug, 1800 UTC 31 Aug, 0600 UTC 2 Sep 2004
Ivan	1200 UTC 9 Sep, 0000 UTC 11 Sep, 0000 UTC 12 Sep, 0600 UTC 14 Sep, 1800 UTC 15 Sep 2004
Katrina	1800 UTC 28 Aug 2005
Rita	0600 UTC 22 Sep 2005
Wilma	1200 UTC 19 Oct 2005
Dean	1200 UTC 18 Aug 2007
Danielle	1800 UTC 27 Aug 2010

best-track intensity evolution following the onset of weakening for each ERC event is used to form a climatology of ERC intensity evolution. In cases of landfall, the data taken while the storm center is over land are omitted. Figure 1 shows the climatology of intensity and intensity change at and after the onset of weakening based on the ERC events and times of onset given in Table 1. Within this sample, most ERC weakening phases begin during periods of high intensity, at a mean intensity of about 135 kt ( $1 \text{ kt} = 0.51 \text{ m s}^{-1}$ ) and within an interquartile intensity range of 120–145 kt. In the first 6 h after the onset of ERC weakening, the mean intensity change is  $-9 \text{ kt}$ ; in the period 6–12 h after onset of weakening, the mean change is  $-6 \text{ kt}$ ; and in the period 12–18 h after the onset of weakening, the mean change is  $-3 \text{ kt}$ . Beyond 18 h, the intensity change is fairly flat and variable, with a small tendency toward continued, but slower, weakening.

The Statistical Hurricane Intensity Prediction Scheme (SHIPS) is a statistical model that provides intensity forecasts based largely on the ambient environmental conditions that the storms move through (e.g., vertical wind shear, sea surface temperature, thermodynamic potential intensity, etc.), and is one of the primary guidance models that the National Oceanic and Atmospheric Administration/National Hurricane Center (NOAA/NHC) uses for their operational intensity forecasts (DeMaria et al. 2005). When the SHIPS intensity forecasts are analyzed during ERCs, however, large errors can emerge.

Figures 2 and 3 compare operational SHIPS intensity change forecasts to the observed intensity evolution following ERCs. In Fig. 2, which is based on 12-hourly SHIPS data, the mean observed weakening in the first

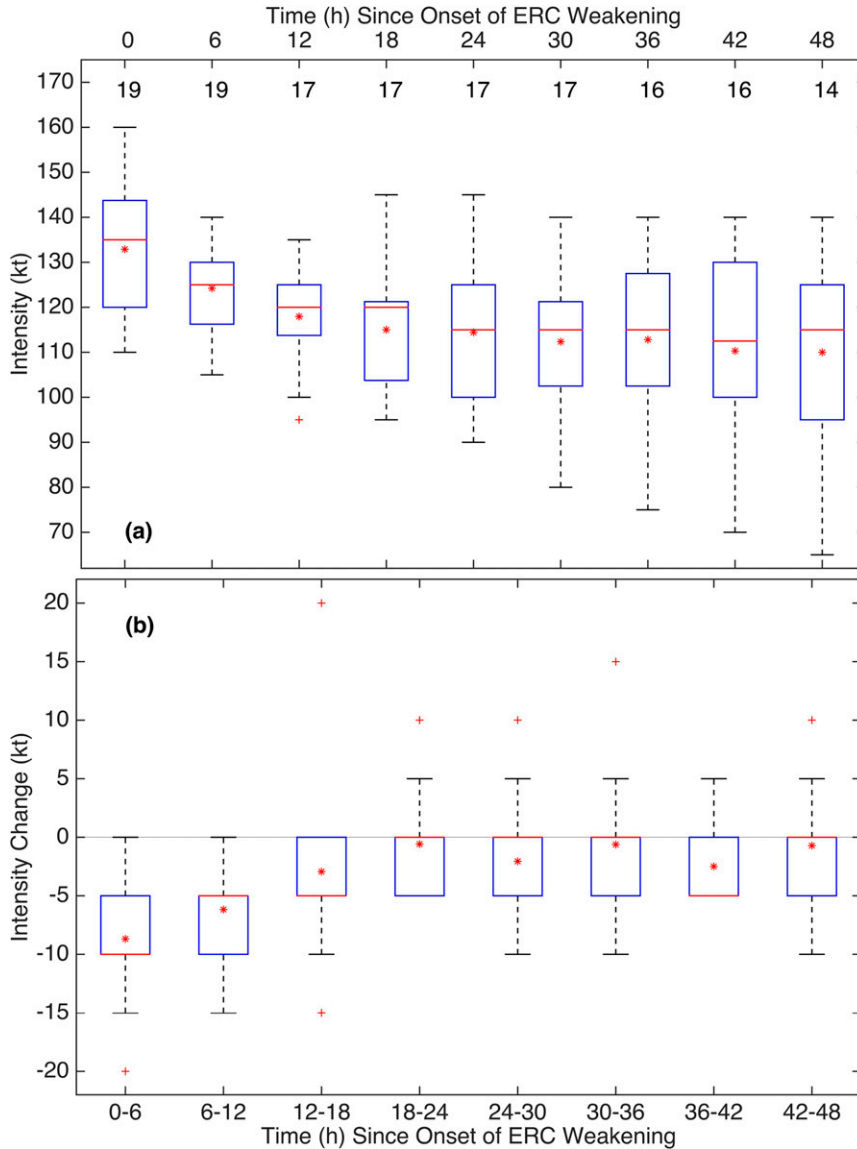


FIG. 1. Climatology of (a) intensity and (b) 6-hourly intensity change from the onset of ERC weakening out to 48 h, based on the recon-anchored best-track dataset during the 19 ERC events shown in Table 1 (values in kt). Red asterisks denote mean values, red lines denote medians, and the blue boxes denote the 25th–75th percentiles of the samples. The whiskers span roughly 99% of the data in each sample, and the red crosses are outliers. Annotated integer values in (a) denote the sample size at that time. Sample size decreases at longer lead times as storms make landfall.

12 h after ERC weakening begins is  $-15$  kt, with an interquartile range from about  $-20$  to  $-10$  kt, while the 12-h SHIPS forecast in this period predicts essentially no intensity change. In the period 12–24 h from the time of onset of ERC weakening, SHIPS provides forecasts of intensity change that are much closer to the observed changes, although the observations show a stronger tendency for continued, but slower, weakening. Beyond 24 h, the mean observed and predicted intensity changes

have roughly converged. However, while the SHIPS intensity change predictions converge toward observations after 24 h, the errors in the first 24 h after ERC lead to large errors in the SHIPS predictions of actual intensity, and these errors are propagated forward into all forecast lead times. Figure 3, which provides 6-hourly intensity changes but is limited to only the most recent ERC events in the sample (Table 1), again shows strong weakening in the observations that is concurrent with

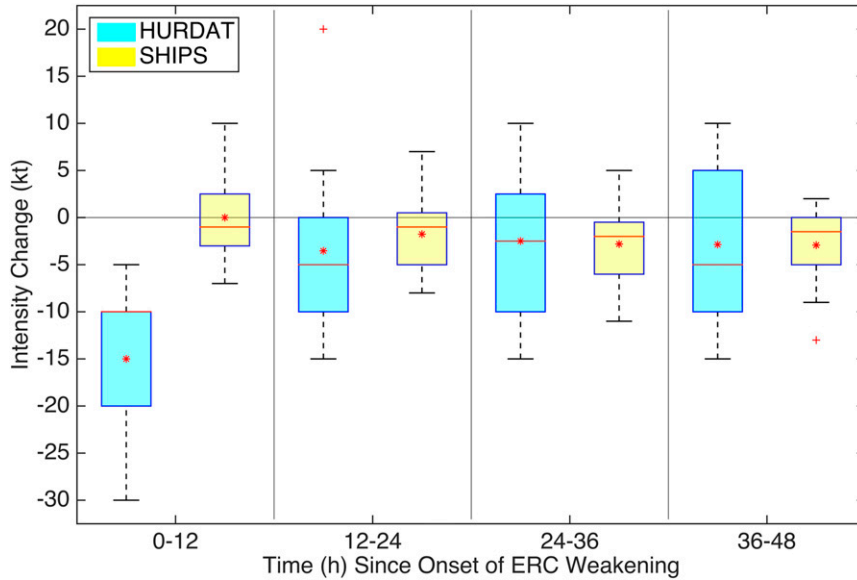


FIG. 2. Comparison of 12-h intensity change in recon-anchored best-track (HURDAT) vs SHIPS predictions following the onset of ERC weakening, based on the 19 ERC events in Table 1.

either slow intensification or a steady state predicted by SHIPS. The disparity is particularly large in the first 12 h and becomes smaller through the following 12 h.

The disparity between SHIPS forecasts and the observed intensity changes during ERCs is strongly suggestive that the typical environmental controls of intensity change, on which SHIPS is largely based, are temporarily countermanded while dynamic processes internal to the storm dominate the intensity evolution. To address this issue, an alternative model is introduced

here that can be applied during ERCs as a complement to SHIPS. The model is based on the climatology of intensity change following onset of ERC weakening, as shown in Fig. 1b and discussed above, and simply reduces intensity by 9, 6, 3, and 1 kt in the 0–6-, 6–12-, 12–18-, and 18–24-h periods after the onset of weakening, respectively. Determining the time of onset in an operational setting poses some challenge, which will be discussed further below. The model is applied using the operational best estimate of current intensity and simply

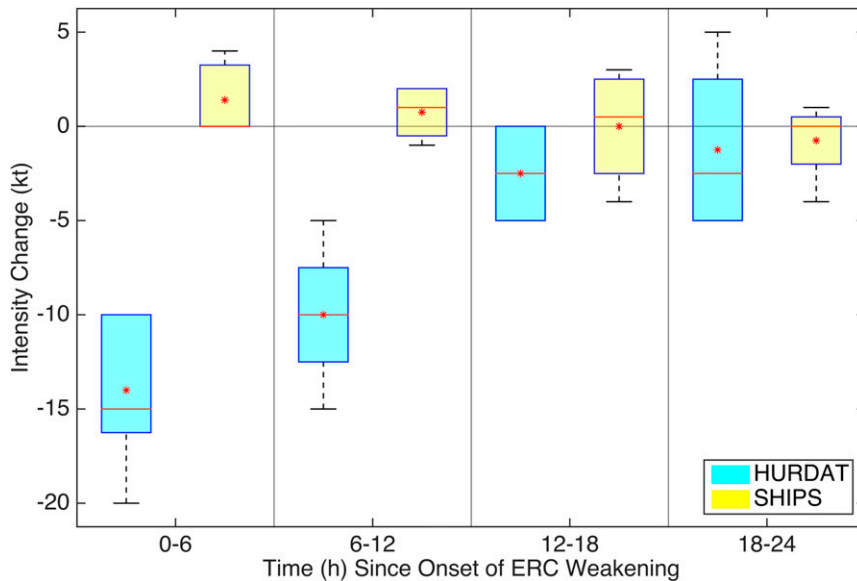


FIG. 3. As in Fig. 2, but using the 6-hourly data available for the five ERC events from Katrina (2005) through Danielle (2010) in Table 1.

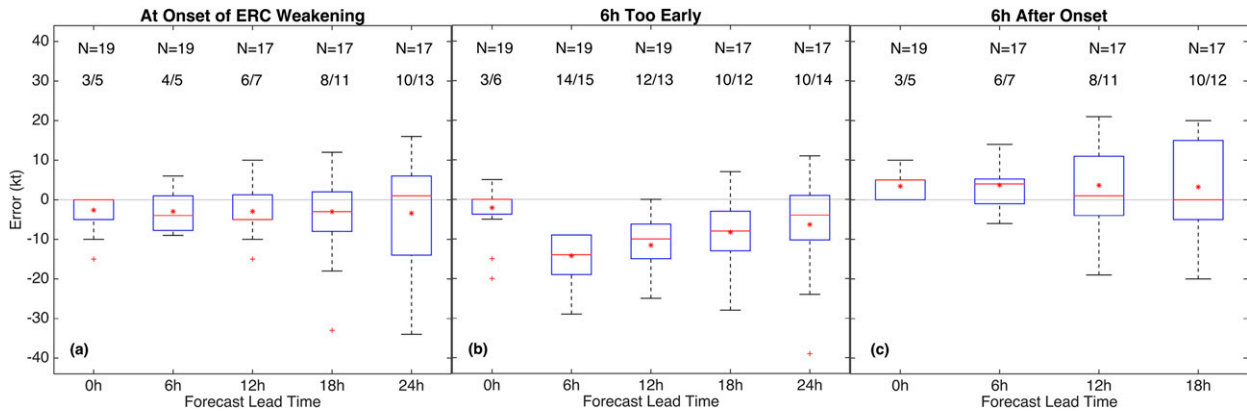


FIG. 4. Error distributions (in kt) for the ERC climatology model, (a) from onset of ERC weakening to 24 h after, (b) error distributions when the model is applied too early (6 h prior to the onset of weakening), and (c) when the model is applied 6 h after the onset of weakening. Errors are relative to recon-anchored best-track values. Positive (negative) values denote where the model-predicted intensities are higher (lower) than the best-track data. Sample size  $N$  is shown for each forecast lead time. MAE and root-mean-square error (RMSE) are shown as MAE/RMSE pairs (in kt).

projects the climatology forward in time. The reduction of intensity by 9, 6, 3, and 1 kt in the four 6-h periods following the onset of ERC weakening is based on the mean values of the sample (red asterisks in Fig. 1b). Another choice that could be made here is to form the climatology with the median values, which would give reductions in intensity of 10, 5, 5, and 0 kt during those periods. We could also form a climatology based on the percentage change of current intensity at the onset of weakening, but since these initial intensities lie within a fairly narrow range in our sample, the difference between using an absolute change or a relative change is small. Ultimately, given our small sample size, there is not much objective justification for making one choice over another, and the differences would be small. We choose to base the climatology model on the mean nonrelative intensity changes for the sake of parsimony.

Figure 4a shows the model errors at various lead times when the model is applied to the full sample of 19 ERC events. Note that since the climatology is based on the full sample of 19 events, the tests shown here and below are dependent tests. Removing a single event has a mostly minimal effect on the climatology, however, and applying a leave-one-event-out cross-validation approach does not significantly impact the error statistics. Still, the sample is fairly small and may not be an optimal representation of a more complete sample of ERC events, in which case it should be understood that the errors shown here may exhibit biases of either sign. More importantly, the errors shown in Fig. 4a are based on the best-case scenario in which the forecaster knows that weakening is about to occur. This could conceivably happen when the forecaster has access to multiple data sources providing information that an ERC is about to

take place, but it may be unlikely that this level of confidence would occur often. Indeed, the penalty for applying the ERC climatology model too early (or when an ERC is not actually taking place at all) is fairly large, as shown in Fig. 4b, and, not surprisingly, substantial underprediction of intensity can occur. A more realistic scenario may be that the forecaster has evidence that an ERC is occurring, and there are clear signs of weakening since the previous 6-hourly forecast cycle. This would also provide the forecaster with an additional 6 h for other evidence of an ERC to become available from microwave satellite or radar imagery, or aircraft reconnaissance data. The errors associated with this scenario are shown in Fig. 4c. The errors are uniformly higher than those in Fig. 4a, as expected, but the penalty is much smaller than in the case of applying the model too early (Fig. 4b). This suggests that the better use of the ERC climatology model in terms of balancing potential gains and penalties would be to apply the model in the following 6-hourly forecast cycle after the onset of ERC weakening has been observed.

Figure 5 compares the ERC climatology model to SHIPS. As in Fig. 4, the error characteristics are shown for the case where the model is applied at the time of onset of ERC weakening (Fig. 5a), 6 h too soon (Fig. 5b), and 6 h after the onset of weakening (Fig. 5c). In the case of perfect timing (Fig. 5a), the ERC climatology model has much lower errors than SHIPS through all lead times of the model application (i.e., 0–24 h after onset of weakening). The difference is particularly striking at 18-h lead time when the errors differ by a factor of more than 300% (although this should be interpreted with caution in light of the limited sample size at this lead time). As before, the penalty for applying the model too

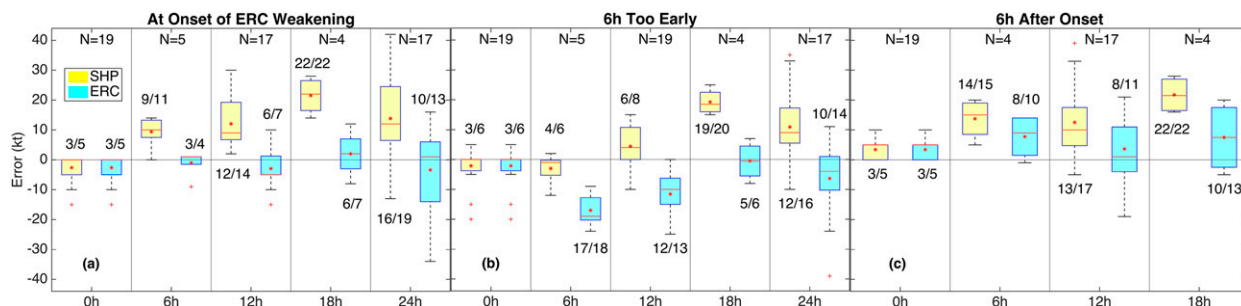


FIG. 5. As in Fig. 4, but comparing the ERC climatology (ERC) model to SHIPS (SHP). For the 19 ERC events, the operational SHIPS data are available with 12-hourly resolution in the pre-2005 storms, and with 6-hourly resolution out to 24-h lead time and 12 hourly at longer lead times for 2005 and later storms.

early is initially large (Fig. 5b), although the errors of the ERC climatology model become smaller than the SHIPS errors at and beyond 18-h lead time. The more realistic application at 6 h past ERC weakening (Fig. 5c) shows larger errors than the perfect timing scenario, as expected, but there is still a significant reduction compared with SHIPS, with mean absolute errors reduced by more than 50% at 18-h lead time (again with the caveat that this value is based on a limited sample size).

The intensity forecast errors during ERC weakening can also be compared to a larger sample of errors. Here, we consider the error statistics of both SHIPS and the official NHC intensity forecasts (obtained from the NHC official forecast error database; <http://www.nhc.noaa.gov/verification/>). For the period 2005–14, and only considering major hurricanes (intensity of 100 kt or greater), the mean absolute errors (MAEs) of the official forecasts at 12- and 24-h forecast lead times are 11 and 16 kt, respectively, and the forecast biases (i.e., mean error) are 5 and 10 kt, respectively. For our 19 ERC cases, the official MAEs at 12 and 24 h forecast lead times are 13 and 18 kt, respectively, and the forecast biases are also 13 and 18 kt, respectively. Performing the same analysis, but using SHIPS forecasts alone, the MAEs for major hurricanes during the period 2005–14 at 12- and 24-h forecast lead times are 12 and 15 kt, respectively, and the forecast biases are 3 and 7 kt, respectively. For our 19 ERC cases, the SHIPS MAEs at 12- and 24-h forecast lead times are 12 and 16 kt, respectively, and the forecast biases are 12 and 14 kt, respectively. Within the limitations of these comparisons, the 12- and 24-h forecast MAEs of the ERC sample are not significantly different from the larger sample, but there is a clear difference in the forecast bias (mean error), as there is a pronounced and consistent overprediction of intensity during these events in both the official forecasts and the SHIPS forecasts.

The ERC climatology model is designed to capture the transient weakening that is observed during ERCs

but is not captured by SHIPS because the weakening generally occurs in an environment that is conducive to intensification (or steady state). However, the convergence of the observed and predicted intensity changes at lead times beyond 24 h after the onset of ERC weakening (Figs. 2 and 3) suggests that the environmental control of intensity change that was temporarily countermanded is mostly restored after this time. This behavior is analogous to landfall cases, in which the usual environmental controls of intensity change are temporarily dominated by land effects such as changes in friction and latent heat exchange. In these cases, the SHIPS forecasts are replaced with specialized predictions provided by Decay-SHIPS (Kaplan and DeMaria 1995; DeMaria et al. 2005; DeMaria et al. 2014). Decay-SHIPS (D-SHIPS) temporarily takes control of the intensity evolution until the storm reemerges over water (if it does at all), after which the environmental control is handed back and the usual SHIPS intensity change predictions are applied. The ERC climatology model is designed to be applied in the same way, although the onset of ERC weakening is significantly harder to predict, or even diagnose (e.g., Kossin and Sitkowski 2009), than landfall. When this is done, the ERC climatology model can provide forecasts out to the same lead times as SHIPS and, in effect, simply adjusts the SHIPS intensity forecasts by a constant factor at all lead times beyond 24 h after onset of ERC weakening. For naming consistency with D-SHIPS then, we will refer to the ERC climatology model as E-SHIPS.

A comparison of the mean D-SHIPS and E-SHIPS forecasts is shown in Fig. 6 for the 16 of 19 ERC events that were not interrupted by landfall within 24 h after onset of weakening. The colored lines in Fig. 6 show the average forecast values over these 16 ERC events, and the black line shows the average best-track intensities from 18 h prior to onset of ERC weakening to 66 h after. The forecasts are shown for the time of onset of weakening, and for the following three 6-hourly forecast



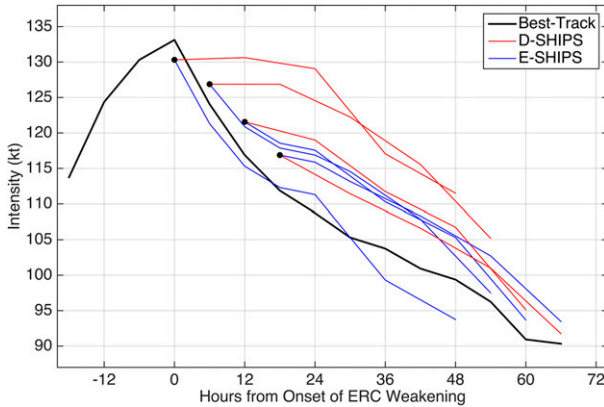


FIG. 6. Operational D-SHIPS (red) and E-SHIPS (blue) forecasts at the onset of ERC weakening and in the following three 6-hourly forecast cycles after the onset. Black dots show the mean operational best estimates of current intensity for the four forecast cycles.

cycles. The initial errors, as seen by the vertical distance between the black dots and the black line, show the errors in the operational estimate of current intensity compared to the postseason analyzed intensities that become the best track. At the onset of weakening ( $t = 0$  h), D-SHIPS predicts little change in intensity, which causes a large overprediction in intensity that extends to 48-h lead time and beyond. Similar D-SHIPS errors occur in the following forecast cycle, 6 h after the onset of weakening. In the following forecast cycle, 12 h after the onset of weakening, the D-SHIPS and E-SHIPS errors are more comparable but with E-SHIPS still providing somewhat smaller errors at 6–12-h lead time. In the next forecast cycle, 18 h after onset, the D-SHIPS result actually has smaller errors than E-SHIPS, although this is largely due to the high bias of the operational best estimate of current intensity for that forecast cycle.

Noting also from Fig. 6 that the onset of ERC weakening is associated with a clear reversal of intensification

rate that the forecaster would be aware of 6 h after onset, the most plausible and effective forecast cycles for application of the E-SHIPS, then, are the three cycles 6–18 h after the onset of weakening. Application of E-SHIPS at the time of onset could clearly reduce intensity forecast errors further, but this would require a high level of confidence that an ERC is under way, perhaps before clear and persistent signs of weakening emerge. Still, the NHC forecast specialists do have operational access to a model that provides a probability that an ERC is beginning (Kossin and Sitkowski 2009), and there may be occasions when weakening is evident since the last forecast cycle but before the next cycle arrives. Furthermore, evidence of a developing secondary wind maximum is often observed by aircraft reconnaissance prior to the onset of weakening (Sitkowski et al. 2011), and there can be additional signs of an impending ERC that manifest in satellite microwave imagery. In these cases, the forecast specialist may have the confidence to apply the model for four consecutive forecast cycles.

E-SHIPS has been selected for operational implementation at NOAA’s NHC, and is presently being transitioned to operations as a subalgorithm that runs within SHIPS. An example of the present form of model output is shown in Table 2 and provides the forecast specialist with a choice of when ERC weakening occurred, or will occur. This choice allows the forecast specialist to apply the model according to the time since the onset of weakening as well as providing some foresight into how intensity may evolve if an ERC occurs in the near future.

### 3. Summary

Hurricane eyewall replacement cycles pose a unique challenge to operational intensity forecasting because the intensity evolution during these cycles is apparently driven mostly by vortex-scale processes that are

TABLE 2. Present format of the ERC climatology model (E-SHIPS) output applied within SHIPS. Forecast lead times span 0–120 h. All other values are intensity (kt). Values at lead time = 0 are the operational best estimates of current intensity for this forecast cycle. In cases when the onset of ERC weakening occurred 24 h ago, the ERC climatology model forecasts are identical to D-SHIPS.

Lead time (h)	0	6	12	18	24	36	48	60	72	84	96	108	120
D-SHIPS forecast	115	115	118	121	122	122	122	113	109	103	92	52	46
E-SHIPS forecasts													
Onset of ERC weakening													
24 h ago	115	115	118	121	122	122	122	113	109	103	92	52	46
18 h ago	115	114	117	120	121	121	121	112	108	102	91	51	45
12 h ago	115	112	111	114	115	115	115	106	102	96	85	45	39
6 h ago	115	109	106	105	106	106	106	97	93	87	76	36	30
Now	115	106	100	97	96	96	96	87	83	77	66	26	20
In 6 h	115	115	106	100	97	95	95	86	82	76	65	25	19
In 12 h	115	115	118	109	103	99	99	90	86	80	69	29	23

internally regulated. This is in contrast to the more common aspects of intensity evolution in which the external (ambient) environment that the storm moves through plays the key role. Since SHIPS, which is a primary intensity guidance model for NOAA's NHC, depends largely on the relationship between the evolution of intensity and the ambient environment, the transient but large intensity excursions during an ERC are not captured by the model and thus can introduce substantial error into operational intensity forecasts. This is somewhat analogous to cases when storms interact temporarily with land (e.g., passage over a large island or a peninsula), and the usual environmental controls of intensity are countermanded by other factors related to the land interaction. As these storms reemerge into open water, the usual environmental controls are restored. For ERC cases, the usual environmental controls of intensity are restored, on average, after about 18–24 h after the onset of weakening occurred. Here, we introduced a model designed to specifically address the transient deficiencies of SHIPS during ERCs. The model, named E-SHIPS, is based on a simple climatology of intensity changes observed in 19 ERC events and is being transitioned into NOAA's NHC operations as a subalgorithm of SHIPS, with the tenable prospect that it will contribute to reducing operational intensity forecast errors.

As a closing note, as operational numerical weather prediction (NWP) models have become increasingly sophisticated, internal hurricane vortex dynamics have become better represented. Indeed, operational NWP models, such as the Hurricane Weather Research and Forecasting (HWRF) Model, have been shown to produce ERCs in idealized settings as well as hindcast settings (e.g., [Zhu et al. 2015](#) and references therein). It is not yet clear, however, how these advancements will be ultimately utilized in operational forecasts. ERCs may be unique among internal vortex dynamical processes, in that they apparently behave as discrete short-lived events, rather than as part of a continuum of internal processes that contribute, for example, to the intensification process (e.g., [Montgomery and Smith 2014](#) and references therein). Thus, in addition to the primary challenge of simply generating a realistic ERC, the operational NWP models (or model ensembles) must also capture the timing of onset and subsequent duration of the ERC. Given the transient nature of the intensity fluctuations associated with ERCs, accurate timing is essential, which poses a significant challenge to NWP model development as well as model interpretation in an operational setting.

*Acknowledgments.* Funding and support for the development of this statistical intensity forecast model was provided by the Joint Hurricane Testbed Project within NOAA's U.S. Weather Research Program (USWRP). We are especially grateful to Chris Landsea and a number of National Hurricane Center specialists for their input and guidance.

#### REFERENCES

- DeMaria, M., M. Mainelli, L. K. Shay, J. A. Knaff, and J. Kaplan, 2005: Further improvements in the Statistical Hurricane Intensity Prediction Scheme (SHIPS). *Wea. Forecasting*, **20**, 531–543, doi:[10.1175/WAF862.1](#).
- , C. R. Sampson, J. A. Knaff, and K. D. Musgrave, 2014: Is tropical cyclone intensity guidance improving? *Bull. Amer. Meteor. Soc.*, **95**, 387–398, doi:[10.1175/BAMS-D-12-00240.1](#).
- Kaplan, J., and M. DeMaria, 1995: A simple empirical model for predicting the decay of tropical cyclone winds after landfall. *J. Appl. Meteor.*, **34**, 2499–2512, doi:[10.1175/1520-0450\(1995\)034<2499:ASEMFP>2.0.CO;2](#).
- Knaff, J. A., D. P. Brown, J. Courtney, G. M. Gallina, and J. L. Beven II, 2010: An evaluation of Dvorak technique-based tropical cyclone intensity estimates. *Wea. Forecasting*, **25**, 1362–1379, doi:[10.1175/2010WAF2222375.1](#).
- Knapp, K. R., M. C. Kruk, D. H. Levinson, H. J. Diamond, and C. J. Neumann, 2010: The International Best Track Archive for Climate Stewardship (IBTrACS): Unifying tropical cyclone best track data. *Bull. Amer. Meteor. Soc.*, **91**, 363–376, doi:[10.1175/2009BAMS2755.1](#).
- Kossin, J. P., and M. Sitkowski, 2009: An objective model for identifying secondary eyewall formation in hurricanes. *Mon. Wea. Rev.*, **137**, 876–892, doi:[10.1175/2008MWR2701.1](#).
- , and —, 2012: Predicting hurricane intensity and structure changes associated with eyewall replacement cycles. *Wea. Forecasting*, **27**, 484–488, doi:[10.1175/WAF-D-11-00106.1](#).
- Landsea, C. W., and J. L. Franklin, 2013: Atlantic hurricane database uncertainty and presentation of a new database format. *Mon. Wea. Rev.*, **141**, 3576–3592, doi:[10.1175/MWR-D-12-00254.1](#).
- Montgomery, M. T., and R. K. Smith, 2014: Paradigms for tropical cyclone intensification. *Aust. Meteor. Oceanic J.*, **64**, 37–66.
- Sitkowski, M., J. P. Kossin, and C. M. Rozoff, 2011: Intensity and structure changes during hurricane eyewall replacement cycles. *Mon. Wea. Rev.*, **139**, 3829–3847, doi:[10.1175/MWR-D-11-00034.1](#).
- Velden, C., and Coauthors, 2006: The Dvorak tropical cyclone intensity estimation technique: A satellite-based method that has endured for over 30 years. *Bull. Amer. Meteor. Soc.*, **87**, 1195–1210, doi:[10.1175/BAMS-87-9-1195](#).
- Willoughby, H. E., J. A. Clos, and M. Shoreibah, 1982: Concentric eye walls, secondary wind maxima, and the evolution of the hurricane vortex. *J. Atmos. Sci.*, **39**, 395–411, doi:[10.1175/1520-0469\(1982\)039<0395:CEWSWM>2.0.CO;2](#).
- Zhu, P., and Coauthors, 2015: Impact of subgrid-scale processes on eyewall replacement cycle of tropical cyclones in HWRF system. *Geophys. Res. Lett.*, **42**, 10 027–10 036, doi:[10.1002/2015GL066436](#).